Measurements of single top-quark production with the ATLAS detector

Philipp Sturm[*]

On behalf of the ATLAS Collaboration
University of Wuppertal
E-mail: philipp.sturm@cern.ch

We present the measurement of the single top-quark t-channel production and evidence for the associated production of a W boson together with a top-quark in proton-proton collisions at $\sqrt{s} = 7\,\text{TeV}$ recorded with the ATLAS detector at the Large Hadron Collider. The t-channel production cross-section is measured using $1.04\,\text{fb}^{-1}$ of collision data. The cross-section is measured by fitting the distribution of a neural network, yielding $\sigma_t = 83 \pm 4\,(\text{stat.})^{+20}_{-19}\,(\text{syst.})\,\text{pb}$ in good agreement with the prediction of the Standard Model. Using the measured cross-section to extract $|V_{tb}|$ and assuming $|V_{tb}| \gg |V_{td}|, |V_{ts}|$ a result of $|V_{tb}| = 1.13^{+0.14}_{-0.13}$ is obtained. Under the assumption of $0 < |V_{tb}| < 1$ a lower limit of $|V_{tb}| > 0.75$ is set at the 95% confidence level. We also present the measurement of the ratio of the top-quark and antitop-quark production in the t-channel $R_t = 1.81 \pm 0.10\,(\text{stat.})^{+0.21}_{-0.20}\,(\text{syst.})$ using $4.7\,\text{fb}^{-1}$. We present evidence for the Wt production in the dileptonic final state analysing $2.01\,\text{fb}^{-1}$ of collision data. The Wt production cross-section is determined by fitting the distribution of a multivariate discriminant constructed with a BDT, yielding $\sigma_{Wt} = 16.8 \pm 2.9\,(\text{stat.}) \pm 4.9\,(\text{syst.})\,\text{pb}$ in good agreement with the Standard Model expectation. The observed sensitivity of the measurement is 3.4σ. From the cross-section measurement the CKM matrix element $|V_{tb}| = 1.03^{+0.16}_{-0.19}$ is derived under the assumption that $|V_{tb}| \gg |V_{td}|, |V_{ts}|$.

---

[*]Speaker.

1. Introduction

At hadron colliders three different processes of the single-top-quark production involving the W-t-b vertex are distinguished. The t-channel and s-channel are characterised by the exchange of a virtual W boson and the associated production (Wt) by the production of a top quark together with a real W boson. The predicted cross-sections at the LHC at $\sqrt{s} = 7\,\text{TeV}$ are $64.6^{+2.7}_{-2.0}\,\text{pb}$ for the t-channel [1], $15.7 \pm 1.1\,\text{pb}$ for the associated production [2], and $4.6 \pm 0.2\,\text{pb}$ for the s-channel [3]. The final state of the single top-quark production provides a direct probe of the W-t-b coupling and is sensitive to many models of new physics [4]. Additionally, the single top-quark and single top-antiquark production cross-section, $\sigma_t(t)$ and $\sigma_t(\bar{t})$ in the t-channel are sensitive to the u-quark and d-quark parton density distribution (PDF) of the proton.

This report presents an analysis measuring the single top-quark t-channel production cross-section in the semi-leptonic decay channel and one analysis establishing evidence of the single top-quark associated production in the dileptonic decay channel.

2. Event Reconstruction

Electron candidates are required to have $E_T > 25\,\text{GeV}$ and $|\eta_{\text{cl}}| < 2.47$. Here, $|\eta_{\text{cl}}|$ denotes the pseudorapidity of the calorimeter cluster. The electron candidate has to obey stringent quality criteria on the properties of the electron track and the associated calorimeter cluster. Also, the electron needs to be well isolated [5]. Muon candidates are reconstructed by combining track segments found in the inner detector and muon spectrometer. They are required to have $p_T > 25\,\text{GeV}$ and $|\eta| < 2.5$. Quality criteria on the tracks and a stringent isolation criteria have to be fulfilled by selected muon candidates [10] . Jets are reconstructed using the anti-k_T algorithm with a radius parameter of 0.4. The response of the calorimeter is corrected by p_T- and η-dependent factors [6, 7, 8]. Jets originating from a b-quark are identified in the region $|\eta| < 2.5$ by reconstructing secondary and tertiary vertices from the tracks associated with each jet and combining life-time related information with a neural network (NN) [9].

3. Measurement of single top quark t-channel cross section

Selected events require exactly one good charged lepton, electron or muon, $E_T^{\text{miss}} > 25\,\text{GeV}$. Reconstructed jets need to have $p_T > 25\,\text{GeV}$ and $|\eta| < 4.5$. Events having two or three jets, among which exactly one is identified as originating from a b quark are considered. The main backgrounds to the single top-quark final state are multijet events in which one of the jets is misidentified as a lepton. These contributions are reduced by $m_T(W) > (60\,\text{GeV} - E_T^{\text{miss}})$. Other important backgrounds are the production of a W boson in association with jets and $t\bar{t}$ production. Smaller backgrounds such as Z+jets, diboson production, single top-quark Wt-channel and s-channel production, as well as $t\bar{t}$ production are normalised to their theoretical predictions. The normalisation of the multijet background is obtained using a binned maximum-likelihood fit to the E_T^{miss}-distribution, before the E_T^{miss} cut, using a data-derived template for the multijet background and templates from Monte-Carlo simulations for all other processes. The kinematic distributions of the W+jets background comprises contributions from W+heavy flavour jets ($Wb\bar{b}$+jets, $Wc\bar{c}$+jets and Wc+jets) and

W+light jets are taken from simulated event samples. The normalisation of the flavour composition is determined simultaneously while fitting the NN output discriminant to measure the *t*-channel single top quark rate.

To separate *t*-channel single top-quark signal events from background several kinematic observables are combined to one discriminant by employing a NN. In the 2-jet dataset 12 variables are used. The most discriminating variables are the invariant mass of the *b*-tagged jet, the charged lepton, and the reconstructed neutrino (using a *W* boson mass constrain) $m_{\ell vb}$, the pseudorapidity of the untagged jet $|\eta(j_u)|$ and the transverse energy of the untagged jet $E_{\mathrm{T}}(j_u)$. In the 3-jet dataset 18 variables are needed for a sufficient separation of signal events and background. The most important discriminating observables are the invariant mass of the two leading jets $m(j_1 j_2)$, $m_{\ell vb}$, and the absolute value of the difference in the pseudorapidity of the leading and lowest p_{T} jet $|\Delta\eta(j_1, j_3)|$. The distribution of the NN discriminant is shown in Fig. 1. To extract the number of signal events, a combined binned maximum-likelihood fit of the NN discriminant in the 2-jet and 3-jet datasets is performed. Systematic uncertainties affect the shape of the NN discriminant and the normalisation of the signal and backgrounds. Both, the rate and shape uncertainties are taken into account by generating correlated pseudo-experiments. The impact of the systematic uncertainties on the measurement is estimated from these pseudo-experiments. Uncertainties on the object modelling, the Monte Carlo generators, the PDFs, the theoretical cross-sections, the background normalisation to data, and integrated luminosity are considered.
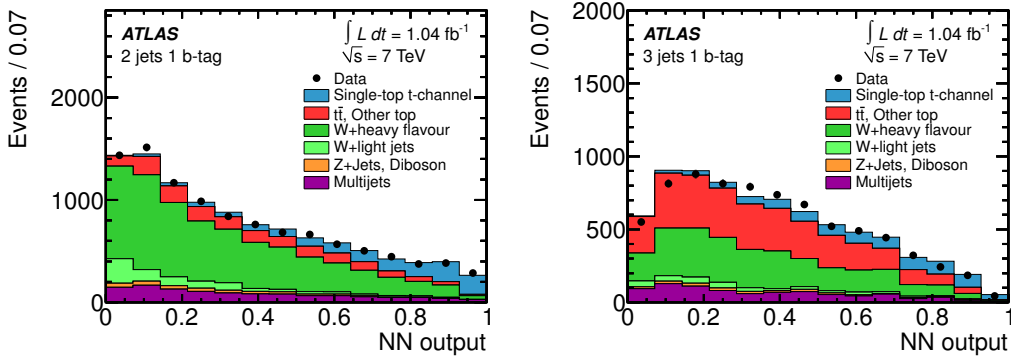

Figure 1: Distribution of the NN discriminant in the 2-jet dataset (left) and 3 jet dataset (right) normalised to the result of the binned maximum-likelihood fit result [11].

The measurement yields a cross-section of $\sigma_t = 83 \pm 4(\mathrm{stat.})^{+20}_{-19}(\mathrm{syst.})\,\mathrm{pb}$ for the single top-quark *t*-channel production. The significance of the observed signal corresponds to 7.2 standard deviations (6.0 expected) [11].

As a cross-check to the NN analysis, a cut-based analysis is carried out. Additional selection cuts are applied on $|\eta(j_u)| > 2$, $150\,\mathrm{GeV} < m(\ell vb) < 190\,\mathrm{GeV}$ and $H_{\mathrm{T}}(\ell, jets, E_{\mathrm{T}}^{\mathrm{miss}}) > 210\,\mathrm{GeV}$, where H_{T} is the scalar sum of the charged lepton ℓ the missing transverse momentum and the p_{T} of the jets in the event. Additionally in the 2-jet dataset $|\Delta\eta(b, j_u)| > 1$ and in the 3-jet dataset $m_{(j_1 j_2 j_3)} > 450\,\mathrm{GeV}$ is required. This analysis yields a cross-section of $92^{+29}_{-26}\,\mathrm{pb}$.

We also report the measurement of the cross-sections of single top-quark and single top-antiquark production, $\sigma_t(t)$ and $\sigma_t(\bar{t})$ in the *t*-channel, and a measurement of the cross-section ratio

$R_t \equiv \sigma_t(t)/\sigma_t(\bar{t})$ [13] at a center-of-mass energy of $\sqrt{s} = 7\,\text{TeV}$ with $4.7\,\text{fb}^{-1}$. The measurements of $\sigma_t(t)$, $\sigma_t(\bar{t})$ and R_t are sensitive to the PDFs of the u-quark and the d-quark in the momentum fraction range of 0.02 to 0.5.

The analysis follows the same approach as the NN cross-section measurement reported above, with the modification that the analysis is performed in four independent channels: ℓ^+ and ℓ^- for two and three jets. To extract the signal content of the selected sample, we perform a simultaneous maximum likelihood fit to all four NN output distributions. The measured t-channel single top-quark production cross section is $\sigma_t(t) = 53.2 \pm 1.7\,(\text{stat.}) \pm 10.6\,(\text{syst.})\,\text{pb}$, while the top-antiquark production cross section is $\sigma_t(\bar{t}) = 29.5 \pm 1.5\,(\text{stat.}) \pm 7.3\,(\text{syst.})\,\text{pb}$. This results into a measured cross-section ratio of $R_t = 1.81 \pm 0.10\,(\text{stat.})\,^{+0.21}_{-0.20}\,(\text{syst.})$. Figure 2 compares the measured value of R_t to the predictions obtained with different PDF sets.
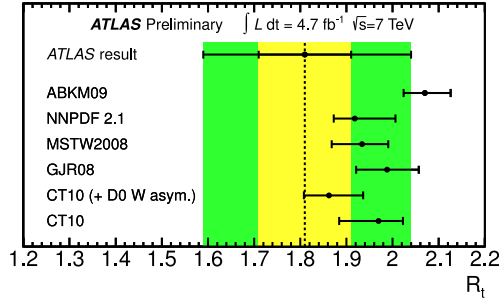

Figure 2: Measurement of R_t with its statistical (yellow band) and total (green band) uncertainty compared to the calculated values for different NLO PDF sets [13].

4. Evidence for Wt production

Selected events are required to contain an opposite sign ee, $\mu\mu$, or $e\mu$ charged lepton pair and at least one jet. Only jets having $p_{\text{T}} > 30\,\text{GeV}$ and $|\eta| < 2.5$ are considered. Identifying jets originating from a b-quark does not offer a significant rejection of the primary background from $t\bar{t}$ events. Signal events feature two neutrinos from the leptonic W boson decay. Thus $E_{\text{T}}^{\text{miss}} > 50\,\text{GeV}$ is required. To reduce the contamination from Z boson decays, the invariant mass of the charged lepton pair must satisfy $81\,\text{GeV} < m_{\ell\ell} < 101\,\text{GeV}$. Additionally, a cut on the sum of the two angles in the transverse plane between each lepton and the missing transverse momentum direction $(\Delta\phi(\ell_1, E_{\text{T}}^{\text{miss}}) + \Delta\phi(\ell_2, E_{\text{T}}^{\text{miss}})) > 2.5$ is applied to reduce the background from $Z \to \tau\tau$ events. Signal events are mainly expected in events featuring one jet. Events having more jets are used as control regions to normalise the backgrounds.

The main background originates from $t\bar{t}$ production in the dilepton final state. The normalisation is estimated from Monte Carlo simulations and constraint by fitting the 2-jet and ≥ 3-jet dataset. Diboson events featuring one jet from initial state radiation make up about 15% of the background events. The background from Z+jets production is determined by data driven methods by defining six signal and background enriched regions for the ee and $\mu\mu$ final state. Addition-

ally, the background from W/Z+jets events with one real lepton and one jet being misidentified as charged lepton are normalised by using the data driven matrix method.

The Wt-channel signal events are discriminated from background by employing a boosted decision tree (BDT). For each, the 1-jet, the 2-jet dataset and for events featuring at least 3 jets, one BDT is trained. The most powerful discriminating observables used in the training are the magnitude of the vectorial sum of the p_T of the leading jet, leptons and missing transverse momentum defined as $p_\mathrm{T}^\mathrm{sys}$, and the ratio $p_\mathrm{T}^\mathrm{sys}/\sqrt{H_\mathrm{T}+\Sigma E_\mathrm{T}}$, where H_T is the scalar sum of the two leptons and the leading jet transverse momenta, and ΣE_T the scalar sum of the transverse energies of all energy deposits in the calorimeter. The distribution of the BDT in the 1-jet and 2-jet dataset is shown in Fig. 3.
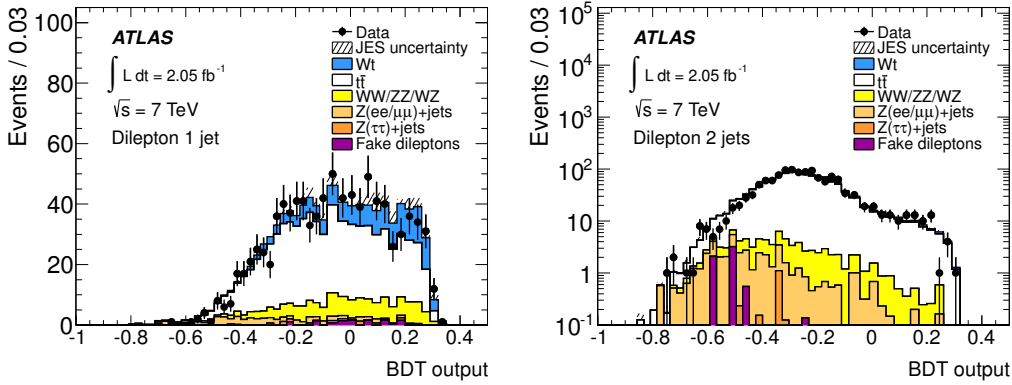

Figure 3: Distribution of the BDT discriminant in the 1-jet dataset (left) and 2 jet dataset (right) normalised to the result of the binned maximum-likelihood fit result [12].

To extract the single top-quark Wt-channel production cross-section a combined template fit of the BDT output distributions for 1-jet, 2-jet and $\geq$ 3-jet events is performed. Both, the rate and shape uncertainties are taken into account by generating correlated pseudo-experiments. The impact of the systematic uncertainties on the measurement is estimated from these pseudo-experiments. Uncertainties on the object modeling, the Monte Carlo generators, the PDFs, the theoretical cross-sections, the background normalisation to data, and integrated luminosity are considered. The Wt-channel production cross-section is measured to be $\sigma_{Wt} = 16.8 \pm 2.9(\mathrm{stat.}) \pm 4.9(\mathrm{syst.})\,\mathrm{pb}$. The sensitivity of the measurement is estimated by employing pseudo experiments. The expected significance assuming the SM expectation is 3.4σ, the observed significance is 3.3σ. The cross-section measurement is used to determine the CKM matrix element $|V_\mathrm{tb}| = 1.03^{+0.16}_{-0.19}$ [12] under the assumption that $|V_{tb}| \gg |V_{td}|, |V_{ts}|$.

5. Summary

We presented a measurement of the single top-quark t-channel production and evidence for the Wt production with the ATLAS detector in pp collisions at $\sqrt{s} = 7\,\mathrm{TeV}$.

The t-channel production cross-section measurement uses $1.04\,\mathrm{fb}^{-1}$ of collision data. Selected events feature one charged lepton, missing transverse momentum, and two or three jets. Exactly

one of the jets is required to origin from a b quark. The cross-section measurement is based on fitting a NN discriminant yielding to $\sigma_t = 83 \pm 4 \text{(stat.)}^{+20}_{-19} \text{(syst.)}$ pb. The corresponding coupling at the W-t-b vertex is $|V_{tb}| = 1.13^{+0.14}_{-0.13}$. A lower limit of $|V_{tb}| > 0.75$ at the 95% C.L. is found.

We also reported the measurement of the single top-quark and single antitop-quark production cross section using 4.7fb^{-1} of collision data. The measurement obtains $\sigma_t(t) = 53.2 \pm 1.7 \text{(stat.)} \pm 10.6 \text{(syst.)}$ pb and $\sigma_t(\bar{t}) = 29.5 \pm 1.5 \text{(stat.)} \pm 7.3 \text{(syst.)}$ pb, yielding a measured cross-section ratio of $R_t = 1.81 \pm 0.10 \text{(stat.)}^{+0.21}_{-0.20} \text{(syst.)}$.

The evidence of the single top-quark production in the Wt channel in the dileptonic decay channel with at least one jet was presented using 2.05fb^{-1} of collision data. A cross-section of $\sigma_{Wt} = 16.8 \pm 2.9 \text{(stat.)} \pm 4.9 \text{(syst.)}$ pb is found. The observed sensitivity of the measurement is 3.3σ, whereas the expected sensitivity is 3.4σ. From the cross-section measurement the CKM matrix element $|V_{tb}| = 1.03^{+0.16}_{-0.19}$ is derived under the assumption of $|V_{tb}| \gg |V_{td}|, |V_{ts}|$.

References

[1] N. Kidonakis, *Next-to-next-to-leading-order collinear and soft gluon corrections for t-channel single top quark production*, Phys. Rev. **D83** (2011) 091503, `arXiv:1103.2792[hep-ph]`.

[2] N. Kidonakis, *Two-loop soft anomalous dimensions for single top quark associated production with a W- or H-*, Phys. Rev. **D82** (2010) 054018, `arXiv:1005.4451[hep-ph]`.

[3] N. Kidonakis, *NNLL resummation for s-channel single top quark production*, Phys. Rev. **D81** (2010) 054028, `arXiv:1001.5034[hep-ph]`.

[4] T. M. Tait and C.-P. Yuan, *Single top quark production as a window to physics beyond the standard model*, Phys.Rev. **D63** (2000) 014018, `arXiv:hep-ph/0007298 [hep-ph]`.

[5] ATLAS Collaboration, "Electron performance measurements with the ATLAS detector using the 2010 LHC proton-proton collision data", Eur. Phys. J. C **72** (2012) 1909, `arXiv:1110.3174 [hep-ex]`.

[6] W. Lampl, *et al.*, "Calorimeter clustering algorithms: Description and performance", ATL-LARG-PUB-2008-002, `https://cds.cern.ch/record/1369219`.

[7] M. Cacciari, G. P. Salam and G. Soyez, "The Anti-k(t) jet clustering algorithm", JHEP **0804** (2008) 063, `arXiv:0802.1189 [hep-ph]`.

[8] ATLAS Collaboration, "Jet energy measurement with the ATLAS detector in proton-proton collisions at $\sqrt{s} = 7$ TeV", `arXiv:1112.6426 [hep-ex]`.

[9] ATLAS Collaboration, "Commissioning of the ATLAS high-performance b-tagging algorithms in the 7 TeV collision data", ATLAS-CONF-2011-102, `https://cds.cern.ch/record/1369219`.

[10] Atlas Collaboration, "Measurement of the $W \to \ell\nu$ and $Z/\gamma^* \to \ell\ell$ production cross sections in proton-proton collisions at $\sqrt{s} = 7$ TeV with the ATLAS detector", JHEP **1012** (2010) 060, `arXiv:1010.2130 [hep-ex]`.

[11] ATLAS Collaboration, "Measurement of the t-channel single top-quark production cross section in pp collisions at $\sqrt{s} = 7$ TeV with the ATLAS detector", Physics Letters B **717** (2012) 330, `arXiv:1205.3130 [hep-ex]`.

[12] ATLAS Collaboration, "Evidence for the associated production of a W boson and a top quark in ATLAS at $\sqrt{s} = 7$ TeV", Phys. Lett. B **716** (2012) 142, `arXiv:1205.5764 [hep-ex]`.

[13] ATLAS Collaboration, "Measurement of the t-channel single top-quark and top-antiquark production cross-sections and their ratio in pp collisions at $\sqrt{s} = 7$ TeV", ATLAS-CONF-2012-056 (2012), https://cdsweb.cern.ch/record/1453783.